

# Protect Measurement-Induced Phase Transition from Noise

Dongheng Qian<sup>1,2</sup> and Jing Wang<sup>1,2,3,4,\*</sup>

<sup>1</sup>State Key Laboratory of Surface Physics and Department of Physics, Fudan University, Shanghai 200433, China

<sup>2</sup>Shanghai Research Center for Quantum Sciences, Shanghai 201315, China

<sup>3</sup>Institute for Nanoelectronic Devices and Quantum Computing, Fudan University, Shanghai 200433, China

<sup>4</sup>Hefei National Laboratory, Hefei 230088, China

(Dated: June 21, 2024)

Measurement-induced phase transition (MIPT) is a novel non-equilibrium phase transition characterized by entanglement entropy. The scrambling dynamics induced by random unitary gates can protect information from low-rate measurements. However, common decoherence noises, such as dephasing, are detrimental to the volume law phase, posing a significant challenge for observing MIPT in current noisy intermediate-scale quantum devices. Here, we demonstrate that incorporating quantum-enhanced operations can effectively protect MIPT from environmental noise. The conditional entanglement entropy is associated with a statistical mechanics model wherein noise and quantum-enhanced operations act as two competing external random fields. Then we show that an *average* apparatus-environment exchange symmetry ensures the conditional entanglement entropy is a valid probe of entanglement. Furthermore, we provide numerical evidence on a (2+1)-d quantum circuit under dephasing noise, demonstrating that MIPT can indeed be observed with the aid of quantum-enhanced operations. This result not only serves as a concrete example of the power of quantum enhancement in combating noise but also holds experimental relevance, as the protocol is straightforward to implement in practice.

Noise presents one of the most significant threats to reliable quantum computation and the long-term storage of quantum information. To address this challenge, quantum error correction (QEC) techniques are employed [1–3]. The core idea of QEC is to encode quantum information in a noise-resilient manner, allowing errors induced by noise to be effectively detected and corrected. The encoding schemes and correction procedures in QEC are typically highly structured [4, 5].

In recent years, measurement-induced phase transitions (MIPT) have attracted significant attention [6–29]. MIPTs can be understood from the perspective of QEC, where information is encoded in an unstructured way through scrambling by random unitary gates, with measurements identified as sources of noise [30]. When the measurement rate is low, corresponding to a low error rate, the entanglement entropy of the state follows a volume law, indicating that the information remains protected. Although this transition has been demonstrated in several experiments [31–34], a major obstacle to observing this transition is its instability against various decoherence noises. It has been shown that the state obeys an area law even with an infinitesimal rate of dephasing noise or resetting noise in the circuit’s bulk [35–38]. This can be interpreted as the scrambling dynamics being insufficient to protect quantum information against these more common practical noises. Therefore, it is both experimentally relevant and theoretically interesting to find a way to protect MIPT from decoherence noise.

Meanwhile, quantum-enhanced (QE) operation has emerged as a potentially more powerful and flexible method for extracting information about a quantum state compared to traditional projective measurements, which only allow access to classical information [39–42]. The

fundamental idea of quantum enhancement is to use a quantum sensor, rather than a classical sensor, to detect the system. It has been demonstrated that an exponential speedup can be achieved in certain tasks by coherently manipulating these quantum probes [39]. However, it remains an open question whether these QE operations and algorithms can maintain their advantage in the presence of noise.

In this Letter, we demonstrate that the original MIPT can be protected against decoherence caused by environmental noise through QE operations. From the perspective of QEC, these QE operations act as an unstructured protocol to protect quantum information by encoding it within both the system qubits and the ancilla qubits.

We first provide analytical analysis, mapping the random quantum circuit to a statistical-mechanics model. We find that noise and QE operation exactly map to two symmetry-breaking fields in different directions. Combining with unitary gate and measurement, we obtain a random field model with ferromagnetic coupling that supports a ferromagnetic-paramagnetic phase transition with both increasing temperature and increasing random field strength. Next, we discover that an *average* apparatus-environment exchange (aAEE) symmetry ensures the conditional entanglement entropy (CEE) to be a valid probe of entanglement [43, 44]. By imposing the aAEE symmetry, we conduct numerical studies for (2+1)-d circuits and explicitly demonstrate the MIPT in the presence of various decoherence noises. Our approach is inspired by Ref. [43], where a prototype setting was introduced. The structure we introduced here incorporates measurement and is much easier to implement in practice, as will be further elaborated later.

*Circuit model.* We consider a quantum circuit where

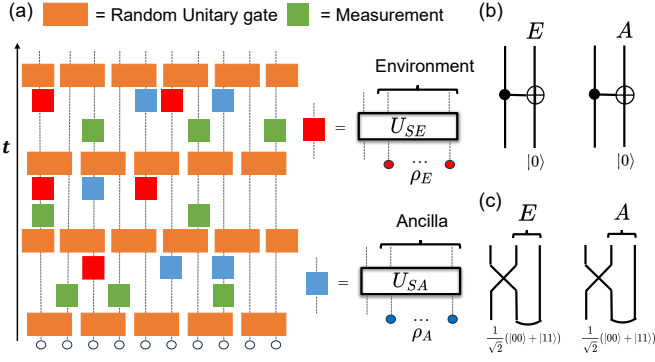


FIG. 1. Circuit structure and operations. (a) The quantum circuit model we consider in this work. Orange, green, red, and blue rectangles represent random unitary gates, measurements, noise, and QE operations, respectively. Noise and QE operation are further detailed as interactions with environment and ancilla qubits. (b) Dephasing noise and the corresponding symmetric QE operation.  $U_{SE} = U_{SA} = \text{CNOT}$  and  $\rho_E = \rho_A = |0\rangle\langle 0|$ . (c) Depolarizing noise and the corresponding symmetric QE operation. Notice that it requires two environment qubits to represent the noise.  $U_{SE} = U_{SA} = \text{SWAP}$ .  $\rho_E$  and  $\rho_A$  are in two-qubit Bell state.

four types of operations are allowed: random unitary gate, measurement, noise, and QE operation. As shown in Fig. 1(a), the unitary gates are applied in a brick wall pattern. Between every two unitary layers, each qubit has a probability  $p$  of being measured projectively. Meanwhile, noise or QE operations occur with probabilities  $q_n$  and  $q_e$ , respectively. Although noises are usually represented as quantum channels, we can adopt the Stinespring representation of the channel to represent it by unitary operations. Specifically, a quantum channel acting on the system can be written as  $\mathcal{N}(\rho) = \text{Tr}_E(U_{SE}(\rho \otimes \rho_E)U_{SE}^\dagger)$  where  $U_{SE}$  represents the interaction between the system and environment, and  $\rho_E$  is the initial state of the environment [45]. In the left column of Fig. 1(b) and 1(c), we show two examples of representing dephasing and depolarizing noise from this perspective. Similarly, QE operations can be considered as applying a unitary  $U_{SA}$  to entangle the system with the ancilla qubits, whose initial states are  $\rho_A$ . We provide representative examples in the right column of Fig. 1(b) and 1(c). It's worth noticing that the number of environment and ancilla qubits are not limited. Despite the similarity in the diagrams, it is crucial to emphasize that the environment qubits are always discarded at the end, signifying that the information is inevitably lost by tracing out these qubits. In contrast, the ancilla qubits remain under our control, allowing us to have full access to and manipulation of them.

The input global state can be written as  $|\Psi_0^{ESA}\rangle = |\psi_E\rangle \otimes |\psi_S\rangle \otimes |\psi_A\rangle$  and a certain realization can be regarded as acting unitary gates and projection oper-

ators on it. At the end of every realization  $m$ , the global state can be represented as an unnormalized pure state  $|\Psi_m^{ESA}\rangle$  and the physically relevant state is  $\rho_m^{SA} = \text{Tr}_E(|\Psi_m^{ESA}\rangle\langle\Psi_m^{ESA}|)$ . For convenience, we drop the superscript from now on. In this work, the realization  $m$  includes both the circuit structure resulting from the random gates and operation locations, as well as the trajectory labeling by different measurement outcomes.

*Analytical analysis.* Instead of considering subsystem entanglement entropy, we aim to calculate the CEE  $\overline{S(M|A)} \equiv \overline{S(M, A)} - \overline{S(A)}$ . The overline here represents averaging all circuits and measurement outcomes. Mathematically, this can be expressed as,

$$\begin{aligned} \overline{S(M|A)} &= \lim_{n \rightarrow 1} (\overline{S^{(n)}(M, A)} - \overline{S^{(n)}(A)}) \\ &= \lim_{n \rightarrow 1} \lim_{k \rightarrow 0} \frac{1}{(1-n)k} \log \left( \frac{\mathcal{Z}_{MA}^{(n,k)}}{\mathcal{Z}_A^{(n,k)}} \right) \\ &= \lim_{n \rightarrow 1} \lim_{k \rightarrow 0} \frac{1}{(n-1)k} \left( \mathcal{F}_{MA}^{(n,k)} - \mathcal{F}_A^{(n,k)} \right), \end{aligned} \quad (1)$$

where

$$\begin{aligned} \mathcal{Z}_{MA}^{(n,k)} &= \sum_m \text{Tr} \left( \mathbb{C}^M \Lambda_A^{(n,k)} \right), \quad \mathcal{Z}_A^{(n,k)} = \sum_m \text{Tr} \left( \Lambda_A^{(n,k)} \right), \\ \Lambda_A^{(n,k)} &= \text{Tr}_{A \cup E} \left[ (|\Psi_m\rangle\langle\Psi_m|)^{\otimes Q} \mathbb{C}^A \right]. \end{aligned} \quad (2)$$

$\mathcal{F}^{n,k} = -\log \mathcal{Z}^{(n,k)}$  is identified as the free energy [46]. The underlying statistical-mechanics model for  $\mathcal{Z}^{(n,k)}$  is composed of spins that take values in the permutation group  $\mathbb{S}(Q)$  with  $Q = nk + 1$ . We designate the iden-

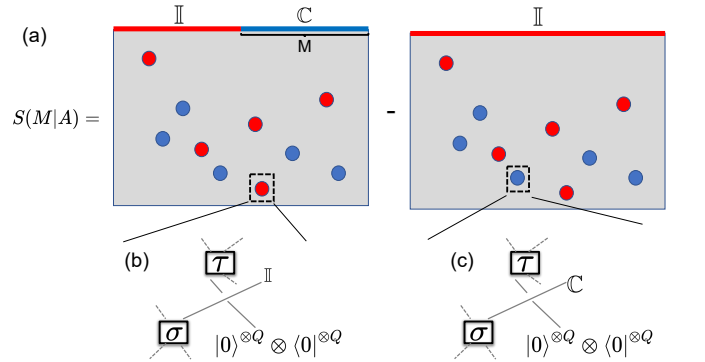


FIG. 2. Statistical-mechanics model. (a)  $\overline{S(M|A)}$  is equal to the free energy difference of the same random field model under different boundary conditions. Red and blue color represents  $\mathbb{I}$  and  $\mathbb{C}$ , respectively. The circles within the bulk indicate that the boundary conditions on environment and ancilla qubits are equivalent to applying extrinsic fields in different directions on the spins. Their locations are random due to the stochastic application of noise and QE operations. (b), (c) Detailed schematics illustrating the bond weight in the statistical-mechanics model, showing a qubit subjected to resetting noise and QE operations.

tity operation in  $\mathbb{S}(Q)$  as  $\mathbb{I}_Q$  and a particular permutation operator as  $\mathbb{C} = \mathbb{S}^{\otimes k} \otimes \mathbb{I}$ .  $\mathbb{S}$  is the cyclic permutation operation in permutation group  $\mathbb{S}(n)$ . Thus,  $S(M|A)$  is related to the free energy difference under different boundary conditions, as shown in Fig. 2(a). In both  $\mathcal{Z}_{MA}$  and  $\mathcal{Z}_A$ , the environment qubits are always subject to the boundary condition  $\mathbb{I}$  while the ancilla qubits are subject to  $\mathbb{C}$ . It has been shown that the entanglement phase transition can be seen as the spontaneous breaking of the  $(\mathbb{S}_Q \times \mathbb{S}_Q) \times \mathbb{Z}_2$  symmetry [47–49]. However, boundary condition imposing on environment qubits can be effectively understood as an explicit symmetry-breaking field in the bulk that align the spins to direction  $\mathbb{I}$ , which is thus detrimental to MIPT [35–37]. Through QE operation and considering the conditional entropy, we effectively introduced another symmetry-breaking field in direction  $\mathbb{C}$  to counteract with the effect of noises. Taking the example of the resetting noise and its associated symmetric QE operation  $U_{SE} = U_{SA} = \text{SWAP}, \rho_E = \rho_A = |0\rangle\langle 0|$ , the bond weight connecting two spins  $\sigma$  and  $\tau$  can be explicitly formulated as [46],

$$W^{\text{reset}}(\sigma, \tau) = (1-p)(1-q) \langle \sigma | \tau \rangle + (1-p) \frac{q}{2} (\langle \sigma | \mathbb{C} \rangle + \langle \sigma | \mathbb{I} \rangle) + pd. \quad (3)$$

We choose  $q_n = q_e = q/2$  which ensures that the total symmetry-breaking field is zero. The model has a  $(\mathcal{C}_{\mathbb{S}_Q}(\mathbb{C}) \times \mathbb{Z}_2) \times \mathbb{Z}_2$  symmetry where  $\mathcal{C}_{\mathbb{S}_Q}(\mathbb{C})$  is the centralizer of  $\mathbb{C}$  [46]. Note that  $\langle \sigma | \tau \rangle = d^{|\sigma\tau^{-1}|}$  where  $d$  is the local Hilbert space dimension and  $|\sigma\tau^{-1}|$  denotes the number of cycles in permutation  $\sigma\tau^{-1}$ . In the  $d \rightarrow \infty$  limit,  $\langle \sigma | \tau \rangle$  becomes  $d^Q \delta_{\sigma, \tau}$ . This corresponds to a random field  $Q$ -state Potts model, where the first term can be interpreted as a ferromagnetic coupling, the second term as two competing random fields, and the final term as the effect of temperature. The strength of the random fields is controlled by  $q$  while temperature is controlled by  $p$ . Given prior work demonstrating phase transitions in random field Ising models and Potts models [50–59], we anticipate that a phase transition would occur at finite  $p$  and  $q$  in quantum circuit which is directly characterized by  $S(M|A)$ . For depolarizing and dephasing noises, the corresponding statistical-mechanics models are analogous as provided in Supplemental Material [46].

*Average symmetry.* Since  $\overline{S(M|A)}$ , as opposed to  $S(M)$  in traditional setting, undergoes a phase transition, it is pertinent to determine under what conditions  $\overline{S(M|A)}$  serves as a valid probe of entanglement or quantum information [60]. It has been proven that if the system has information exchange (IE) symmetry in every realization, such that  $S(M|A) = S(M|E)$ , then  $S(M|A)$  ensures entanglement between  $M$  and  $M^c \cup A$  [44]. Here,  $M^c$  denotes the complement of the subsystem  $M$ . Volume law scaling of  $S(M|A)$  would then yield an extensive number of distillable Bell pairs between  $M$  and  $M^c \cup A$ .

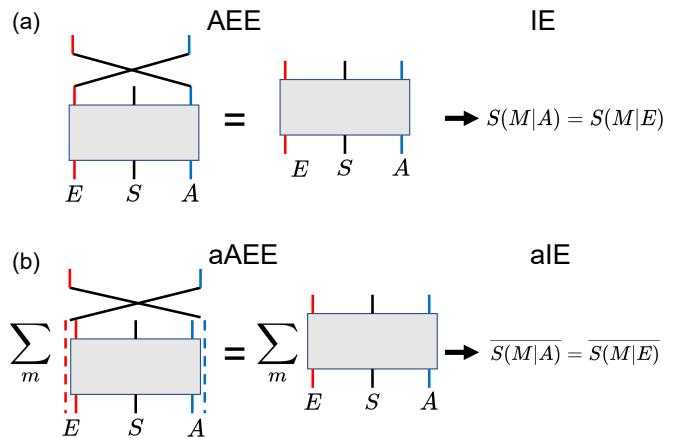


FIG. 3. Relationship between symmetries. (a) AEE symmetry requires that every realization remains invariant under the SWAP operation on environment and ancilla qubits, which consequently leads to IE symmetry. (b) The aAEE symmetry is the averaged version of AEE symmetry. The dashed lines indicate that unentangled qubits can be added to balance the number of qubits before applying the SWAP operation. The aAEE symmetry would then result in an aIE symmetry, which is the averaged version of IE symmetry.

The IE symmetry can be guaranteed if an apparatus-environment exchange (AEE) symmetry is present, which requires that each circuit realization be symmetric under the exchange of ancilla and environment qubits. However, this symmetry is explicitly violated by any realization in our circuit since noise and QE operation are independently chosen and applied at each location. Additionally, the number of ancilla and environment qubits may differ within a specific circuit realization, making the “exchange” operation more subtle to define. To solve this issue, we propose that an aAEE symmetry can still lead to an average IE (aIE) symmetry, thereby making the averaged CEE a valid probe of entanglement. The relationship between these symmetries are summarized in Fig. 3. We first define a generalized SWAP operation  $\text{SWAP}'$  on  $|\Psi_m\rangle$  as initially adding unentangled qubits to either  $E$  or  $A$  to equalize the number of qubits. Subsequently, a conventional SWAP gate is applied to  $E$  and  $A$ , followed by the removal of the unentangled qubits.  $\text{SWAP}'|\Psi_m\rangle$  would not necessarily equal to  $|\Psi_m\rangle$ , but may transform it into another realization  $|\Psi_{m'}\rangle$ . The aAEE symmetry requires that the probabilities of these two realizations occurring are identical. Concretely, one can represent the circuit’s outcome as  $\rho = \sum_m |\Psi_m\rangle\langle\Psi_m|$ , and the aAEE symmetry necessitates that

$$\text{SWAP}'\rho\text{SWAP}'^\dagger = \rho. \quad (4)$$

This is reminiscent of the recently proposed average (weak) symmetry in the study of mixed state order [61–66]. A subtlety in defining  $\rho$  in this manner is that the number of qubits in  $|\Psi_m\rangle$  may vary, but this can be

simply addressed by adding unentangled qubits to states with fewer qubits. With aAEE symmetry and combining with Eq. (2), one would have

$$\sum_m \Lambda_A^Q = \text{Tr}_{A \cup E}(\rho^{\otimes Q} \mathbb{C}^A) = \text{Tr}_{A \cup E} \left( \text{SWAP}' \rho^{\otimes Q} \text{SWAP}'^\dagger \mathbb{C}^A \right) = \text{Tr}_{A \cup E}(\rho^{\otimes Q} \mathbb{C}^E) \equiv \sum_m \Lambda_E^Q. \quad (5)$$

This result implies that  $\overline{S(M|A)} = \overline{S(M|E)}$ , which we call the aIE symmetry. It is then straightforward to show that aIE symmetry results in,

$$\begin{aligned} \overline{S(M|A)} &\geq 0, & \overline{S(M|A)} &= \overline{S(M^c|A)}, \\ \overline{S(M|A)} &= -\overline{S(M|A \cup M^c)}, \end{aligned} \quad (6)$$

which also ensure that  $\overline{S(M|A)}$  represents the entanglement between  $M$  and  $M^c \cup A$ .

Translating the aAEE symmetry into the concrete circuit model reveals that it requires  $\rho_E = \rho_A$ ,  $U_{SE} = U_{SA}$  and  $q_n = q_e = q/2$ . Thus, QE operation should be symmetric with the corresponding noise, and the operation should be applied at the same rate as the noise. It is noteworthy that aAEE symmetry condition  $q_n = q_e$  aligns with the condition of zero net field in the statistical-mechanics model. Since every noise can be represented in the Stinespring form [45], QE operations can protect MIPT from various types of noise.

*Numerical results.* We now turn to numerical calculations to explicitly demonstrate MIPT in the presence of noise and QE operations. Considering the absence of phase transitions in the 2D random field Ising model due to Imry-Ma argument [58], we directly simulate the (2+1)-d quantum circuit with  $L \times L$  qubits on a square lattice, corresponding to a 3D statistical model. To ensure efficient simulation, we choose the random unitary gates to be Clifford gates, allowing the circuit to be simulated using the stabilizer formalism [67–69]. A single time step consists of four random unitary layers [46]. Between every two layers, measurement in  $z$ -basis, noise, and QE operations occur at each site with probabilities  $p$ ,  $q/2$  and  $q/2$ , respectively. In the absence of any noise, MIPT occurs at around  $p \sim 0.3$ . We evolve the circuit for depth  $T = 10L$  to achieve convergence in all simulations and employ the technique proposed in Ref. [43] to perform efficient simulations without storing the ancilla qubits explicitly. In particular, we consider dephasing noise here, and results for other types of noise and additional numerical results can be found in Supplemental Material [46].

To determine the critical point, we consider the conditional tripartite mutual information  $I_3$ . We take periodic boundary condition in both directions and partition the system into four segments with equal size, as depicted in Fig. 4(a).  $I_3$  is expected to scale with  $L$  in the volume law phase, while approach 0 in the area law phase [70, 71].

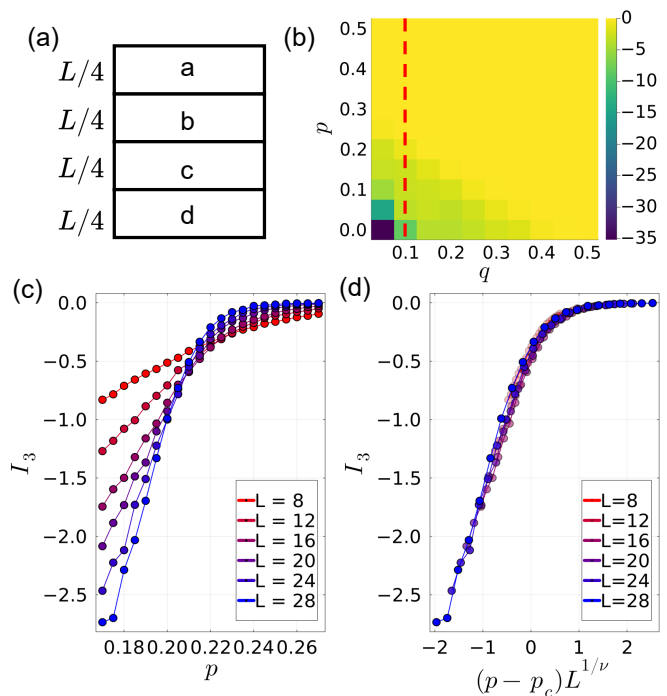


FIG. 4. Numerical results for dephasing noise. (a) We partition the system into four neighboring regions with equal size as a, b, c, d. The conditional tripartite mutual information is then calculated as  $I_3 = S'(a) + S'(b) + S'(c) - S'(ab) - S'(ac) - S'(bc) + S'(abc)$  where  $S'(x) \equiv \overline{S(x|A)}$ . (b)  $I_3$  vs  $(p, q)$  with  $L = 20$ . The red line  $q = 0.1$  is further examined in (c), (d), which demonstrate MIPT in the presence of noise and QE operation. Each data point is averaged over  $5 \times 10^4$  realizations.

The complete phase diagram can thus be constructed by identifying the regions where  $I_3$  is zero or not, as shown in Fig. 4(b), where a volume law phase is clearly observed for non-zero values of  $q$  and  $p$ . We further focus on the line  $q = 0.1$  and collapse the data according to the scaling form  $I_3 = f((p - p_c)L^{1/\nu})$ . The results are shown in Fig. 4(c) and 4(d). The critical point is  $p_c = 0.214(2)$  with the critical exponent  $\nu = 0.9(1)$ , which is close to the result for noiseless case in [71]. Details for data collapse are provided in [46].

*Discussions.* Similar to QEC, where more physical qubits are required to encode a smaller number of logical qubits, our scheme necessitates the preparation of additional ancilla qubits as the circuit depth increases. Specifically,  $O(qNT)$  ancilla qubits are needed, where  $N$  is the number of system qubits,  $p$  is the noise rate, and  $T$  is the circuit depth. Assuming  $q_e \sim 1\%$ ,  $L = 20$  and  $T = 10L$ , around 800 ancilla qubits are needed to observe the phase transition. It is important to highlight that each ancilla qubit is utilized only once and can be isolated after use, thereby mitigating the risk of noise contamination.

An immediate application of our scheme requires prior

knowledge of the probability that a specific type of decoherence noise will occur in the experimental setting. Our scheme can be directly adapted to determine the noise rate as follows: apply a finite amount of measurement such that the state enters the area-law phase, then sweep through different QE operation rates  $q_e$ . In a finite-size system,  $S(M|A)$  will be greater than zero if  $q_e > q_n$  and less than zero otherwise.

Besides noise, post-selection is another significant challenge preventing MIPT from being easily observed. Here the post-selection problem persists when the measurement rate is non-zero because determining the CEE of a single trajectory requires post-selecting on the measurement outcomes, a difficulty rooted in Born's rule. Recent work has utilized various post-selection-free methods to probe the phase transition, such as using cross-entropy benchmarking [72] or providing bounds on the entanglement entropy [73, 74]. We believe these methods can also be extended to the conditional entropy in this work, and we leave this exploration for future work.

Finally, we highlight the differences between our circuit model and that in Ref. [43, 44]. Apart from incorporating measurement in our circuit, the most notable difference is that noise and QE operations act randomly and independently, not necessarily at the same location. The only requirement is that their rates are equal, which serves as a more realistic and feasible setting since we usually cannot accurately predict where and when noise will occur. Additionally, previous work has demonstrated a noise-induced phase transition where the noise rate is inversely proportional to the system size [75]. In our case, the noise rate is constant, which again represents a more realistic scenario.

*Acknowledgment.* We thank Shane P. Kelly for valuable discussions. This work is supported by the National Key Research Program of China under Grant No. 2019YFA0308404, the Natural Science Foundation of China through Grants No. 12350404 and No. 12174066, the Innovation Program for Quantum Science and Technology through Grant No. 2021ZD0302600, the Science and Technology Commission of Shanghai Municipality under Grants No. 23JC1400600 and No. 2019SHZDZX01.

---

\* wjingphys@fudan.edu.cn

- [1] B. Schumacher and M. A. Nielsen, Quantum data processing and error correction, *Phys. Rev. A* **54**, 2629 (1996).
- [2] A. Yu. Kitaev, Quantum Error Correction with Imperfect Gates, in *Quantum Communication, Computing, and Measurement*, edited by O. Hirota, A. S. Holevo, and C. M. Caves (Springer US, Boston, MA, 1997) pp. 181–188.
- [3] A. Y. Kitaev, Fault-tolerant quantum computation by anyons, *Ann. Phys.* **303**, 2 (2003).
- [4] E. Dennis, A. Kitaev, A. Landahl, and J. Preskill, Topological quantum memory, *J. Math. Phys.* **43**, 4452 (2002).
- [5] C. Wang, J. Harrington, and J. Preskill, Confinement-Higgs transition in a disordered gauge theory and the accuracy threshold for quantum memory, *Ann. Phys.* **303**, 31 (2003).
- [6] Y. Li, X. Chen, and M. P. A. Fisher, Measurement-driven entanglement transition in hybrid quantum circuits, *Phys. Rev. B* **100**, 134306 (2019).
- [7] M. J. Gullans and D. A. Huse, Dynamical purification phase transition induced by quantum measurements, *Phys. Rev. X* **10**, 041020 (2020).
- [8] A. Chan, R. M. Nandkishore, M. Pretko, and G. Smith, Unitary-projective entanglement dynamics, *Phys. Rev. B* **99**, 224307 (2019).
- [9] Y. Bao, M. Block, and E. Altman, Finite-Time Teleportation Phase Transition in Random Quantum Circuits, *Phys. Rev. Lett.* **132**, 030401 (2024).
- [10] Y. Bao, S. Choi, and E. Altman, Symmetry enriched phases of quantum circuits, *Ann. Phys.* **435**, 168618 (2021), special issue on Philip W. Anderson.
- [11] S. J. Garratt, Z. Weinstein, and E. Altman, Measurements conspire nonlocally to restructure critical quantum states, *Phys. Rev. X* **13**, 021026 (2023).
- [12] J. Y. Lee, W. Ji, Z. Bi, and M. P. A. Fisher, Decoding measurement-prepared quantum phases and transitions: from ising model to gauge theory, and beyond (2022), [arXiv:2208.11699 \[cond-mat.str-el\]](https://arxiv.org/abs/2208.11699).
- [13] Y. Li, X. Chen, A. W. W. Ludwig, and M. P. A. Fisher, Conformal invariance and quantum nonlocality in critical hybrid circuits, *Phys. Rev. B* **104**, 104305 (2021).
- [14] Y. Li, S. Vijay, and M. P. Fisher, Entanglement domain walls in monitored quantum circuits and the directed polymer in a random environment, *PRX Quantum* **4**, 010331 (2023).
- [15] A. Nahum and B. Skinner, Entanglement and dynamics of diffusion-annihilation processes with majorana defects, *Phys. Rev. Research* **2**, 023288 (2020).
- [16] A. Nahum, S. Vijay, and J. Haah, Operator spreading in random unitary circuits, *Phys. Rev. X* **8**, 021014 (2018).
- [17] A. Nahum, J. Ruhman, S. Vijay, and J. Haah, Quantum entanglement growth under random unitary dynamics, *Phys. Rev. X* **7**, 031016 (2017).
- [18] S. Sharma, X. Turkeshi, R. Fazio, and M. Dalmonte, Measurement-induced criticality in extended and long-range unitary circuits, *SciPost Phys. Core* **5**, 023 (2022).
- [19] S. Sang, Y. Li, T. Zhou, X. Chen, T. H. Hsieh, and M. P. Fisher, Entanglement negativity at measurement-induced criticality, *PRX Quantum* **2**, 030313 (2021).
- [20] B. Skinner, J. Ruhman, and A. Nahum, Measurement-induced phase transitions in the dynamics of entanglement, *Phys. Rev. X* **9**, 031009 (2019).
- [21] M. Szyniszewski, A. Romito, and H. Schomerus, Entanglement transition from variable-strength weak measurements, *Phys. Rev. B* **100**, 064204 (2019).
- [22] R. Vasseur, A. C. Potter, Y.-Z. You, and A. W. W. Ludwig, Entanglement transitions from holographic random tensor networks, *Phys. Rev. B* **100**, 134203 (2019).
- [23] A. Zabalo, M. J. Gullans, J. H. Wilson, S. Gopalakrishnan, D. A. Huse, and J. H. Pixley, Critical properties of the measurement-induced transition in random quantum circuits, *Phys. Rev. B* **101**, 060301 (2020).
- [24] O. Alberton, M. Buchhold, and S. Diehl, Entanglement Transition in a Monitored Free-Fermion Chain: From Ex-

- tended Criticality to Area Law, *Phys. Rev. Lett.* **126**, 170602 (2021).
- [25] L. Fidkowski, J. Haah, and M. B. Hastings, How dynamical quantum memories forget, *Quantum* **5**, 382 (2021).
- [26] M. P. A. Fisher, V. Khemani, A. Nahum, and S. Vijay, Random Quantum Circuits, *Annu. Rev. Condens. Matter Phys.* **14**, 335 (2023).
- [27] I. Poboiko, I. V. Gornyi, and A. D. Mirlin, Measurement-induced phase transition for free fermions above one dimension, *Phys. Rev. Lett.* **132**, 110403 (2024).
- [28] D. Qian and J. Wang, Steering-induced phase transition in measurement-only quantum circuits, *Phys. Rev. B* **109**, 024301 (2024).
- [29] X. Yu and X.-L. Qi, Measurement-induced entanglement phase transition in random bilocal circuits (2022), [arXiv:2201.12704](https://arxiv.org/abs/2201.12704).
- [30] S. Choi, Y. Bao, X.-L. Qi, and E. Altman, Quantum Error Correction in Scrambling Dynamics and Measurement-Induced Phase Transition, *Phys. Rev. Lett.* **125**, 030505 (2020).
- [31] J. C. Hoke, M. Ippoliti, E. Rosenberg, D. Abanin, R. Acharya, T. I. Andersen, M. Ansmann, F. Arute, K. Arya, A. Asfaw, J. Atalaya, J. C. Bardin, A. Bengtsson, G. Bortoli, A. Bourassa, J. Bovaird, L. Brill, M. Broughton, B. B. Buckley, D. A. Buell, T. Burger, B. Burkett, N. Bushnell, Z. Chen, B. Chiaro, D. Chik, J. Cogan, R. Collins, P. Conner, W. Courtney, A. L. Crook, B. Curtin, A. G. Dau, D. M. Debroy, A. D. T. Barba, S. Demura, A. Di Paolo, I. K. Drozdov, A. Dunsworth, D. Eppens, C. Erickson, E. Farhi, R. Fatemi, V. S. Ferreira, L. F. Burgos, E. Forati, A. G. Fowler, B. Foxen, W. Giang, C. Gidney, D. Gilboa, M. Giustina, R. Gosula, J. A. Gross, S. Habegger, M. C. Hamilton, M. Hansen, M. P. Harrigan, S. D. Harrington, P. Heu, M. R. Hoffmann, S. Hong, T. Huang, A. Huff, W. J. Huggins, S. V. Isakov, J. Iveland, E. Jeffrey, C. Jones, P. Juhas, D. Kafri, K. Kechedzhi, T. Khattar, M. Khezri, M. Kieferová, S. Kim, A. Kitaev, P. V. Klimov, A. R. Klots, A. N. Korotkov, F. Kostritsa, J. M. Kreikebaum, D. Landhuis, P. Laptev, K.-M. Lau, L. Laws, J. Lee, K. W. Lee, Y. D. Lensky, B. J. Lester, A. T. Lill, W. Liu, A. Locharla, O. Martin, J. R. McClean, M. McEwen, K. C. Miao, A. Mieszala, S. Montazeri, A. Morvan, R. Movassagh, W. Mruczkiewicz, M. Neeley, C. Neill, A. Nersisyan, M. Newman, J. H. Ng, A. Nguyen, M. Nguyen, M. Y. Niu, T. E. O'Brien, S. Omonije, A. Opremcak, A. Petukhov, R. Potter, L. P. Pryadko, C. Quintana, C. Rocque, N. C. Rubin, N. Saei, D. Sank, K. Sankaragomathi, K. J. Satzinger, H. F. Schurkus, C. Schuster, M. J. Shearn, A. Shorter, N. Shutty, V. Shvarts, J. Skrzuzny, W. C. Smith, R. D. Somma, G. Sterling, D. Strain, M. Szalay, A. Torres, G. Vidal, B. Villalonga, C. V. Heidweiller, T. White, B. W. K. Woo, C. Xing, Z. J. Yao, P. Yeh, J. Yoo, G. Young, A. Zalcman, Y. Zhang, N. Zhu, N. Zobrist, H. Neven, R. Babbush, D. Bacon, S. Boixo, J. Hilton, E. Lucero, A. Megrant, J. Kelly, Y. Chen, V. Smelyanskiy, X. Mi, V. Khemani, and P. Roushan, Measurement-induced entanglement and teleportation on a noisy quantum processor, *Nature* **622**, 481 (2023).
- [32] H. Kamakari, J. Sun, Y. Li, J. J. Thio, T. P. Gujarati, M. P. A. Fisher, M. Motta, and A. J. Minnich, Experimental demonstration of scalable cross-entropy benchmarking to detect measurement-induced phase transitions on a superconducting quantum processor (2024), [arXiv:2403.00938](https://arxiv.org/abs/2403.00938).
- [33] J. M. Koh, S.-N. Sun, M. Motta, and A. J. Minnich, Measurement-induced entanglement phase transition on a superconducting quantum processor with mid-circuit readout, *Nature Phys.* **19**, 1314 (2023).
- [34] C. Noel, P. Niroula, D. Zhu, A. Risinger, L. Egan, D. Biswas, M. Cetina, A. V. Gorshkov, M. J. Gullans, D. A. Huse, and C. Monroe, Measurement-induced quantum phases realized in a trapped-ion quantum computer, *Nature Phys.* **18**, 760 (2022).
- [35] B. C. Dias, D. Perković, M. Haque, P. Ribeiro, and P. A. McClarty, Quantum noise as a symmetry-breaking field, *Phys. Rev. B* **108**, L060302 (2023).
- [36] S. Liu, M.-R. Li, S.-X. Zhang, S.-K. Jian, and H. Yao, Universal KPZ scaling in noisy hybrid quantum circuits, *Phys. Rev. B* **107**, L201113 (2023).
- [37] Z. Weinstein, Y. Bao, and E. Altman, Measurement-Induced Power-Law Negativity in an Open Monitored Quantum Circuit, *Phys. Rev. Lett.* **129**, 080501 (2022).
- [38] S. Liu, M.-R. Li, S.-X. Zhang, and S.-K. Jian, Entanglement structure and information protection in noisy hybrid quantum circuits, *Phys. Rev. Lett.* **132**, 240402 (2024).
- [39] D. Aharonov, J. Cotler, and X.-L. Qi, Quantum algorithmic measurement, *Nature Commun.* **13**, 887 (2022).
- [40] H.-Y. Huang, R. Kueng, and J. Preskill, Information-Theoretic Bounds on Quantum Advantage in Machine Learning, *Phys. Rev. Lett.* **126**, 190505 (2021).
- [41] J. Zhao, J. Dias, J. Y. Haw, M. Bradshaw, R. Blandino, T. Symul, T. C. Ralph, S. M. Assad, and P. K. Lam, Quantum enhancement of signal-to-noise ratio with a heralded linear amplifier, *Optica* **4**, 1421 (2017).
- [42] D. Braun, G. Adesso, F. Benatti, R. Floreanini, U. Marzolino, M. W. Mitchell, and S. Pirandola, Quantum-enhanced measurements without entanglement, *Rev. Mod. Phys.* **90**, 035006 (2018).
- [43] S. P. Kelly and J. Marino, Entanglement transitions in quantum-enhanced experiments (2023), [arXiv:2310.03061](https://arxiv.org/abs/2310.03061).
- [44] S. P. Kelly and J. Marino, Generalizing measurement-induced phase transitions to information exchange symmetry breaking (2024), [arXiv:2402.13271](https://arxiv.org/abs/2402.13271).
- [45] M. A. Nielsen and I. L. Chuang, *Quantum computation and quantum information* (Cambridge university press, 2010).
- [46] See Supplemental Material for technical details.
- [47] Y. Bao, S. Choi, and E. Altman, Theory of the phase transition in random unitary circuits with measurements, *Phys. Rev. B* **101**, 104301 (2020).
- [48] C.-M. Jian, Y.-Z. You, R. Vasseur, and A. W. W. Ludwig, Measurement-induced criticality in random quantum circuits, *Phys. Rev. B* **101**, 104302 (2020).
- [49] T. Zhou and A. Nahum, Emergent statistical mechanics of entanglement in random unitary circuits, *Phys. Rev. B* **99**, 174205 (2019).
- [50] J. Ding and Z. Zhuang, Long range order for random field Ising and Potts models, *Commun. Pure Appl. Math.* **77**, 37 (2024).
- [51] K. Binder, Random-field induced interface widths in Ising systems, *Z. Physik B - Condensed Matter* **50**, 343 (1983).
- [52] J. Ding, F. Huang, and A. Xia, A phase transition and critical phenomenon for the two-dimensional random field Ising model (2023), [arXiv:2310.12141](https://arxiv.org/abs/2310.12141).

- [53] J. F. Fontanari, W. K. Theumann, and D. R. C. Dominguez, Potts model in a random field, *Phys. Rev. B* **39**, 7132 (1989).
- [54] M. Kumar, V. Banerjee, S. Puri, and M. Weigel, Critical behavior of the three-state random-field Potts model in three dimensions, *Phys. Rev. Research* **4**, L042041 (2022).
- [55] T. Nattermann, Theory of the random field ising model, in *Spin glasses and random fields*, edited by A. F. Young (World Scientific, 1998) pp. 277–298.
- [56] H. Nishimori, Potts model in random fields, *Phys. Rev. B* **28**, 4011 (1983).
- [57] H. Rieger and A. P. Young, Critical exponents of the three dimensional random field ising model, *J. Phys. A: Math. Gen.* **26**, 5279 (1993).
- [58] A. Aharony, Y. Imry, and S.-k. Ma, Lowering of Dimensionality in Phase Transitions with Random Fields, *Phys. Rev. Lett.* **37**, 1364 (1976).
- [59] N. G. Fytas and V. Martín-Mayor, Universality in the Three-Dimensional Random-Field Ising Model, *Phys. Rev. Lett.* **110**, 227201 (2013).
- [60] R. Horodecki, P. Horodecki, M. Horodecki, and K. Horodecki, Quantum entanglement, *Rev. Mod. Phys.* **81**, 865 (2009).
- [61] R. Fan, Y. Bao, E. Altman, and A. Vishwanath, Diagnostics of Mixed-State Topological Order and Breakdown of Quantum Memory, *PRX Quantum* **5**, 020343 (2024).
- [62] R. Ma and C. Wang, Average Symmetry-Protected Topological Phases, *Phys. Rev. X* **13**, 031016 (2023).
- [63] R. Ma, J.-H. Zhang, Z. Bi, M. Cheng, and C. Wang, Topological phases with average symmetries: the decohered, the disordered, and the intrinsic (2023), [arXiv:2305.16399](https://arxiv.org/abs/2305.16399).
- [64] P. Sala, S. Gopalakrishnan, M. Oshikawa, and Y. You, Spontaneous strong symmetry breaking in open systems: Purification perspective (2024), [arXiv:2405.02402](https://arxiv.org/abs/2405.02402).
- [65] Y. Bao, R. Fan, A. Vishwanath, and E. Altman, Mixed-state topological order and the errorfield double formulation of decoherence-induced transitions (2023), [arxiv:2301.05687](https://arxiv.org/abs/2301.05687).
- [66] R. Ma and A. Turzillo, Symmetry Protected Topological Phases of Mixed States in the Doubled Space (2024), [arxiv:2403.13280](https://arxiv.org/abs/2403.13280).
- [67] S. Aaronson and D. Gottesman, Improved simulation of stabilizer circuits, *Phys. Rev. A* **70**, 052328 (2004).
- [68] D. Gottesman, The heisenberg representation of quantum computers (1998), [arXiv:quant-ph/9807006](https://arxiv.org/abs/quant-ph/9807006) [quant-ph].
- [69] D. Gottesman, Stabilizer codes and quantum error correction (1997), [arXiv:quant-ph/9705052](https://arxiv.org/abs/quant-ph/9705052) [quant-ph].
- [70] O. Lunt, M. Szyniszewski, and A. Pal, Measurement-induced criticality and entanglement clusters: A study of one-dimensional and two-dimensional Clifford circuits, *Phys. Rev. B* **104**, 155111 (2021).
- [71] P. Sierant, M. Schirò, M. Lewenstein, and X. Turkeshi, Measurement-induced phase transitions in  $(d + 1)$ -dimensional stabilizer circuits, *Phys. Rev. B* **106**, 214316 (2022).
- [72] Y. Li, Y. Zou, P. Glorioso, E. Altman, and M. P. A. Fisher, Cross entropy benchmark for measurement-induced phase transitions, *Phys. Rev. Lett.* **130**, 220404 (2023).
- [73] S. J. Garratt and E. Altman, Probing post-measurement entanglement without post-selection (2023), [arxiv:2304.20092](https://arxiv.org/abs/2304.20092).
- [74] M. McGinley, Postselection-Free Learning of Measurement-Induced Quantum Dynamics, *PRX Quantum* **5**, 020347 (2024).
- [75] S. Liu, M.-R. Li, S.-X. Zhang, S.-K. Jian, and H. Yao, Noise-induced phase transitions in hybrid quantum circuits (2024), [arxiv:2401.16631](https://arxiv.org/abs/2401.16631).